AIP Conference Proceedings

Modeling of full-Heusler alloys within tight-binding approximation: Case study of Fe_2MnAl

Cite as: AIP Conference Proceedings **1862**, 030040 (2017); https://doi.org/10.1063/1.4991144
Published Online: 10 July 2017

A. Azhar, M. A. Majidi, and D. Nanto

View Online
Export Citation

ARTICLES YOU MAY BE INTERESTED IN

Modeling of half-Heusler compound NiMnSb within tight-binding approximation
AIP Conference Proceedings **1862**, 030020 (2017); https://doi.org/10.1063/1.4991124

Theoretical formulation of optical conductivity of $La_{0.7}Ca_{0.3}MnO_3$ exhibiting paramagnetic insulator - ferromagnetic metal transition
AIP Conference Proceedings **1862**, 030025 (2017); https://doi.org/10.1063/1.4991129

Algorithmic implementation of particle-particle ladder diagram approximation to study strongly-correlated metals and semiconductors
AIP Conference Proceedings **1862**, 030029 (2017); https://doi.org/10.1063/1.4991133

© 2017 Author(s).

Modeling of Full-Heusler Alloys within Tight-Binding Approximation: Case Study of Fe_2MnAl

A. Azhar[1], M. A. Majidi[1, a)], and D. Nanto[2]

[1]*Department of Physics, Faculty of Mathematics and Natural Sciences (FMIPA), Universitas Indonesia, Depok 16424, Indonesia*
[2]*Physics Education, Syarif Hidayatullah State Islamic University, Jakarta 15412, Indonesia*

[a)]Corresponding author: aziz.majidi@sci.ui.ac.id

Abstract. Heusler alloys have been known for about a century, and predictions of magnetic moment values using Slater-Pauling rule have been successful for many such materials. However, such a simple counting rule has been found not to always work for all Heusler alloys. For instance, Fe_2CuAl has been found to have magnetic moment of 3.30 μ_B per formula unit although the Slater-Pauling rule suggests the value of 2 μ_B. On the other hand, a recent experiment shows that a non-stoichiometric Heusler compound $Fe_2Mn_{0.5}Cu_{0.5}Al$ possesses magnetic moment of ~4 μ_B, closer to the Slater-Pauling prediction for the stoichiometric compound. Such discrepancies signify that the theory to predict the magnetic moment of Heusler alloys in general is still far from being complete. Motivated by this issue, we propose to do a theoretical study on a full-Heusler alloy Fe_2MnAl to understand the formation of magnetic moment microscopically. We model the system by constructing a density-functional-theory-based tight-binding Hamiltonian and incorporating Hubbard repulsive as well as spin-spin interactions for the electrons occupying the *d*-orbitals. Then, we solve the model using Green's function approach, and treat the interaction terms within the mean-field approximation. At this stage, we aim to formulate the computational algorithm for the overall calculation process. Our final goal is to compute the total magnetic moment per unit cell of this system and compare it with the experimental data.

INTRODUCTION

Heusler alloys, discovered by Fritz Heulser in 1903, are among the most exciting materials because of their magnetic properties despite that they are not made from magnetic elements. For instance, an alloy with the composition of Cu_2MnAl behaves as ferromagnet although none of its constituent elements is magnetic by itself [1, 2]. Generally, full-Heusler alloys with general formula X_2YZ (X and Y are transition metals, and Z is a main group element) are crystallized in the $L2_1$ structure which is composed of four interpenetrating face-centered-cubic (fcc) lattices (Fig. 1). Their atomic positions are described by Wyckoff coordinates as: X (0,0,0), Y (1/4,1/4,1/4), X (1/2,1/2,1/2) and Z (3/4,3/4,3/4) [3, 4]. Graf *et al.* [5] explains that the properties of Heusler compounds are strongly dependent on the atomic order, so a careful analysis is needed to understand the crystal structure-to-property relation of Heusler compounds.

Surprisingly, the magnetic moments of many Heusler compounds can be predicted using Slater-Pauling rule by counting the number of valance electrons, so that for full-Heusler compounds with four atoms per unit cell the magnetic moment follows the formula $m_{X_2YZ} = N_v - 24$ [5]. Recently, Gasi *et al.* [6] found that Fe_2CuAl does not follow the Slater-Pauling rule, but the non-stoichiometric $Fe_2Mn_{0.5}Cu_{0.5}Al$ does [7]. This fact indicates that the theory to predict the magnetic moment of Heusler alloys may still be far from being complete. Motivated by this, we propose to do a theoretical study on a full-Heulser alloy Fe_2MnAl to understand the formation of magnetic moment microscopically using a density-functional-theory-based tight-binding model.

In this study, we model the Fe_2MnAl system by constructing a tight-binding Hamiltonian, whose parameters are obtained through density functional theory (DFT) calculation, incorporating Hubbard repulsive and spin-spin interactions for the electrons occupying the *d*-orbitals. The model is then solved using Green's function approach, with the interaction terms treated within mean-field approximation. Our ultimate goal of study is to compute the magnetic moment per unit cell of this system, compare it with the experimental data, and analyze the result particularly in its relation to the Slater-Pauling rule. As the introductory part of this work, however, in this paper we only present how we formulate the computational algorithm for the overall calculation process.

International Symposium on Current Progress in Mathematics and Sciences 2016 (ISCPMS 2016)
AIP Conf. Proc. 1862, 030040-1–030040-5; doi: 10.1063/1.4991144
Published by AIP Publishing. 978-0-7354-1536-2/$30.00

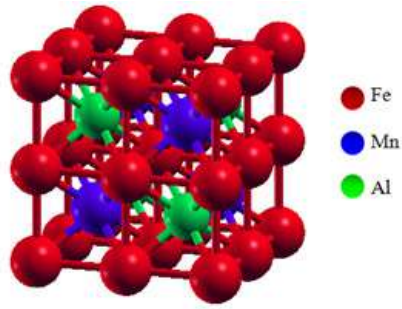

FIGURE 1. Full Heusler alloy Fe_2MnAl crystal structure.

TABLE 1. Basis states for constructing the tight-binding Hamiltonian of full-Heusler Fe_2MnAl.

$\lvert \mathrm{Fe_A} - s\rangle$	$\lvert \mathrm{Fe_A} - d_{xy}\rangle$	$\lvert \mathrm{Fe_A} - d_{xz}\rangle$	$\lvert \mathrm{Fe_A} - d_{yz}\rangle$
$\lvert \mathrm{Fe_A} - d_{z^2}\rangle$	$\lvert \mathrm{Fe_A} - d_{x^2-y^2}\rangle$	$\lvert \mathrm{Fe_B} - s\rangle$	$\lvert \mathrm{Fe_B} - d_{xy}\rangle$
$\lvert \mathrm{Fe_B} - d_{xz}\rangle$	$\lvert \mathrm{Fe_B} - d_{yz}\rangle$	$\lvert \mathrm{Fe_B} - d_{z^2}\rangle$	$\lvert \mathrm{Fe_B} - d_{x^2-y^2}\rangle$
$\lvert \mathrm{Fe_C} - s\rangle$	$\lvert \mathrm{Fe_C} - d_{xy}\rangle$	$\lvert \mathrm{Fe_C} - d_{xz}\rangle$	$\lvert \mathrm{Fe_C} - d_{yz}\rangle$
$\lvert \mathrm{Fe_C} - d_{z^2}\rangle$	$\lvert \mathrm{Fe_C} - d_{x^2-y^2}\rangle$	$\lvert \mathrm{Fe_D} - s\rangle$	$\lvert \mathrm{Fe_D} - d_{xy}\rangle$
$\lvert \mathrm{Fe_D} - d_{xz}\rangle$	$\lvert \mathrm{Fe_D} - d_{yz}\rangle$	$\lvert \mathrm{Fe_D} - d_{z^2}\rangle$	$\lvert \mathrm{Fe_D} - d_{x^2-y^2}\rangle$
$\lvert \mathrm{Fe_E} - s\rangle$	$\lvert \mathrm{Fe_E} - d_{xy}\rangle$	$\lvert \mathrm{Fe_E} - d_{xz}\rangle$	$\lvert \mathrm{Fe_E} - d_{yz}\rangle$
$\lvert \mathrm{Fe_E} - d_{z^2}\rangle$	$\lvert \mathrm{Fe_E} - d_{x^2-y^2}\rangle$	$\lvert \mathrm{Fe_F} - s\rangle$	$\lvert \mathrm{Fe_F} - d_{xy}\rangle$
$\lvert \mathrm{Fe_F} - d_{xz}\rangle$	$\lvert \mathrm{Fe_F} - d_{yz}\rangle$	$\lvert \mathrm{Fe_F} - d_{z^2}\rangle$	$\lvert \mathrm{Fe_F} - d_{x^2-y^2}\rangle$
$\lvert \mathrm{Fe_G} - s\rangle$	$\lvert \mathrm{Fe_G} - d_{xy}\rangle$	$\lvert \mathrm{Fe_G} - d_{xz}\rangle$	$\lvert \mathrm{Fe_G} - d_{yz}\rangle$
$\lvert \mathrm{Fe_G} - d_{z^2}\rangle$	$\lvert \mathrm{Fe_G} - d_{x^2-y^2}\rangle$	$\lvert \mathrm{Fe_H} - s\rangle$	$\lvert \mathrm{Fe_H} - d_{xy}\rangle$
$\lvert \mathrm{Fe_H} - d_{xz}\rangle$	$\lvert \mathrm{Fe_H} - d_{yz}\rangle$	$\lvert \mathrm{Fe_H} - d_{z^2}\rangle$	$\lvert \mathrm{Fe_H} - d_{x^2-y^2}\rangle$
$\lvert \mathrm{Mn_A} - s\rangle$	$\lvert \mathrm{Mn_A} - d_{xy}\rangle$	$\lvert \mathrm{Mn_A} - d_{xz}\rangle$	$\lvert \mathrm{Mn_A} - d_{yz}\rangle$
$\lvert \mathrm{Mn_A} - d_{z^2}\rangle$	$\lvert \mathrm{Mn_A} - d_{x^2-y^2}\rangle$	$\lvert \mathrm{Mn_B} - s\rangle$	$\lvert \mathrm{Mn_B} - d_{xy}\rangle$
$\lvert \mathrm{Mn_B} - d_{xz}\rangle$	$\lvert \mathrm{Mn_B} - d_{yz}\rangle$	$\lvert \mathrm{Mn_B} - d_{z^2}\rangle$	$\lvert \mathrm{Mn_B} - d_{x^2-y^2}\rangle$
$\lvert Mn_C - s\rangle$	$\lvert \mathrm{Mn_C} - d_{xy}\rangle$	$\lvert \mathrm{Mn_C} - d_{xz}\rangle$	$\lvert \mathrm{Mn_C} - d_{yz}\rangle$
$\lvert \mathrm{Mn_C} - d_{z^2}\rangle$	$\lvert \mathrm{Mn_C} - d_{x^2-y^2}\rangle$	$\lvert \mathrm{Mn_D} - s\rangle$	$\lvert \mathrm{Mn_D} - d_{xy}\rangle$
$\lvert \mathrm{Mn_D} - d_{xz}\rangle$	$\lvert \mathrm{Mn_D} - d_{yz}\rangle$	$\lvert \mathrm{Mn_D} - d_{z^2}\rangle$	$\lvert \mathrm{Mn_D} - d_{x^2-y^2}\rangle$
$\lvert \mathrm{Al_A} - s\rangle$	$\lvert \mathrm{Al_A} - p_x\rangle$	$\lvert \mathrm{Al_A} - p_y\rangle$	$\lvert \mathrm{Al_A} - p_z\rangle$
$\lvert \mathrm{Al_B} - s\rangle$	$\lvert \mathrm{Al_B} - p_x\rangle$	$\lvert \mathrm{Al_B} - p_y\rangle$	$\lvert \mathrm{Al_B} - p_z\rangle$
$\lvert \mathrm{Al_C} - s\rangle$	$\lvert \mathrm{Al_C} - p_x\rangle$	$\lvert \mathrm{Al_C} - p_y\rangle$	$\lvert \mathrm{Al_C} - p_z\rangle$
$\lvert \mathrm{Al_D} - s\rangle$	$\lvert \mathrm{Al_D} - p_x\rangle$	$\lvert \mathrm{Al_D} - p_y\rangle$	$\lvert \mathrm{Al_D} - p_z\rangle$

MODEL

The crystal structure of the full-Heusler alloy Fe_2MnAl can be described using Wyckoff coordinates as: Fe (0,0,0), Mn (1/4,1/4,1/4), Fe (1/2,1/2,1/2) and Al (3/4,3/4,3/4). From the 88 valence orbitals involved in the unit cell of Fe_2MnAl listed in Table 1, we define the basis states to construct our tight-binding Hamiltonian that serves as the non-interacting part of our full Hamiltonian.

The full Hamiltonian itself reads as

$$H = \sum_{\vec{k}} \hat{c}_{\vec{k}}^{\dagger} \left[H_0(\vec{k})\right] \hat{c}_{\vec{k}} - J_H \sum_{\zeta,\gamma,\alpha,\beta} \vec{s}_{\gamma,\alpha}^{(\zeta)} \cdot \vec{s}_{\gamma,\beta}^{(\zeta)} + U \sum_{\zeta,\gamma,\alpha} n_{\gamma,\alpha\uparrow}^{(\zeta)} n_{\gamma,\alpha\downarrow}^{(\zeta)}. \quad (1)$$

The first term of Equation 1 denotes the non-interacting or the kinetic part of the Hamiltonian. Here, $\left[H_0(\vec{k})\right]$ is an 88×88 matrix defined in momentum space whose elements are constructed within tight-binding approximation using the above 88 basis states. The elements of the matrix $\left[H_0(\vec{k})\right]$ in Equation 1 can be written as

$$H_{0\ i,j}(\vec{k}) = \epsilon_i \delta_{i,j} - t_{i,j} \sum_{\vec{\delta}_{nn}} e^{-i\vec{k}\cdot\vec{\delta}_{nn}}, \quad (2)$$

where ϵ_i denotes the on-site energy corresponding to the orbital i, $\delta_{i,j}$ a Kronecker delta, $t_{i,j}$ denotes the hopping parameter connecting orbitals i and j between nearest-neighbor atoms, and $\vec{\delta}_{nn}$ represents the nearest neighbor

translation vector. Meanwhile, $\hat{c}_{\vec{k}}^{\dagger}$ ($\hat{c}_{\vec{k}}$) is a row (column) vector whose each of its element contains the creation (annihilation) operators corresponding to each basis orbital.

In the second term of Equation 1, $\sum_{\zeta,\gamma,\alpha,\beta} \vec{s}_{\gamma,\alpha}^{(\zeta)} \cdot \vec{s}_{\gamma,\beta}^{(\zeta)}$ represents the interaction between spins of electrons occupying different *d*-orbitals in the same atom. ζ is index of the unit cell, while γ denotes site having *d*-orbitals in a unit cell. α and β denote components of *d*-orbitals. The dot product of two spin operators, $\vec{s}_\alpha \cdot \vec{s}_\beta$, can be expanded as

$$\vec{s}_\alpha \cdot \vec{s}_\beta = s_{x\alpha} s_{x\beta} + s_{y\alpha} s_{y\beta} + s_{z\alpha} s_{z\beta}. \tag{3}$$

n terms of the creation and annihilation operators and the Pauli matrices, the above spin dot product expands further as

$$\begin{aligned}\vec{s}_\alpha \cdot \vec{s}_\beta = {} & \left(\tfrac{\hbar}{2}\right)^2 \begin{pmatrix} a_{\alpha\uparrow}^\dagger & a_{\alpha\downarrow}^\dagger \end{pmatrix} \begin{pmatrix} 0 & 1 \\ 1 & 0 \end{pmatrix} \begin{pmatrix} a_{\alpha\uparrow} \\ a_{\alpha\downarrow} \end{pmatrix} \begin{pmatrix} a_{\beta\uparrow}^\dagger & a_{\beta\downarrow}^\dagger \end{pmatrix} \begin{pmatrix} 0 & 1 \\ 1 & 0 \end{pmatrix} \begin{pmatrix} a_{\beta\uparrow} \\ a_{\beta\downarrow} \end{pmatrix} + \\ & \left(\tfrac{\hbar}{2}\right)^2 \begin{pmatrix} a_{\alpha\uparrow}^\dagger & a_{\alpha\downarrow}^\dagger \end{pmatrix} \begin{pmatrix} 0 & -i \\ i & 0 \end{pmatrix} \begin{pmatrix} a_{\alpha\uparrow} \\ a_{\alpha\downarrow} \end{pmatrix} \begin{pmatrix} a_{\beta\uparrow}^\dagger & a_{\beta\downarrow}^\dagger \end{pmatrix} \begin{pmatrix} 0 & -i \\ i & 0 \end{pmatrix} \begin{pmatrix} a_{\beta\uparrow} \\ a_{\beta\downarrow} \end{pmatrix} + \\ & \left(\tfrac{\hbar}{2}\right)^2 \begin{pmatrix} a_{\alpha\uparrow}^\dagger & a_{\alpha\downarrow}^\dagger \end{pmatrix} \begin{pmatrix} 1 & 0 \\ 0 & -1 \end{pmatrix} \begin{pmatrix} a_{\alpha\uparrow} \\ a_{\alpha\downarrow} \end{pmatrix} \begin{pmatrix} a_{\beta\uparrow}^\dagger & a_{\beta\downarrow}^\dagger \end{pmatrix} \begin{pmatrix} 1 & 0 \\ 0 & -1 \end{pmatrix} \begin{pmatrix} a_{\beta\uparrow} \\ a_{\beta\downarrow} \end{pmatrix}.\end{aligned} \tag{4}$$

To simplify our further calculation, we choose the *z*-direction to be the direction of the net magnetic moment of the unit cell. Then, upon applying mean-filed approximation, the terms corresponding to the average values of the spin components along the *x*- and *y*-directions vanish. Therefore, the first and second term of Equation 2 vanish accordingly, leaving only the terms corresponding to the *z* components

$$\begin{aligned}\vec{s}_\alpha \cdot \vec{s}_\beta \cong \left(\tfrac{\hbar}{2}\right)^2 \big[& \big(n_{\alpha\uparrow}\langle n_{\beta\uparrow}\rangle + n_{\beta\uparrow}\langle n_{\alpha\uparrow}\rangle - \langle n_{\alpha\uparrow}\rangle\langle n_{\beta\uparrow}\rangle\big) - \\ & \big(n_{\alpha\uparrow}\langle n_{\beta\downarrow}\rangle + n_{\beta\downarrow}\langle n_{\alpha\uparrow}\rangle - \langle n_{\alpha\uparrow}\rangle\langle n_{\beta\downarrow}\rangle\big) - \\ & \big(n_{\alpha\downarrow}\langle n_{\beta\uparrow}\rangle + n_{\beta\uparrow}\langle n_{\alpha\downarrow}\rangle - \langle n_{\alpha\downarrow}\rangle\langle n_{\beta\uparrow}\rangle\big) + \\ & \big(n_{\alpha\downarrow}\langle n_{\beta\downarrow}\rangle + n_{\beta\downarrow}\langle n_{\alpha\downarrow}\rangle - \langle n_{\alpha\downarrow}\rangle\langle n_{\beta\downarrow}\rangle\big)\big],\end{aligned} \tag{5}$$

where $a_\uparrow^\dagger a_\uparrow = n_\uparrow$ ($a_\downarrow^\dagger a_\downarrow = n_\downarrow$) denotes occupation number operator of electron with spin up (down).

The last term of Equation 1 represents Hubbard local repulsive interaction. Similar to our treatment to the second term of Equation 1, we also apply mean-field approximation to this term such that

$$n_{\gamma,\alpha\uparrow} n_{\gamma,\alpha\downarrow} \approx n_{\gamma,\alpha\uparrow}\langle n_{\gamma,\alpha\downarrow}\rangle + n_{\gamma,\alpha\downarrow}\langle n_{\gamma,\alpha\uparrow}\rangle - \langle n_{\gamma,\alpha\uparrow}\rangle\langle n_{\gamma,\alpha\downarrow}\rangle. \tag{6}$$

FORMULATION OF THE METHOD

In the kinetic part of Equation1, the matrix $[H_0(\vec{k})]$ is constructed out of 88 basis orbital states in the Fe_2MnAl unit cell, giving it a structure of

$$[H_0(\vec{k})] = \begin{bmatrix} H_{1,1} & \cdots & H_{1,88} \\ \vdots & \ddots & \vdots \\ H_{88,1} & \cdots & H_{88,88} \end{bmatrix} \tag{7}$$

The parameter values of ϵ_i and $t_{i,j}$ defining each element of $[H_0(\vec{k})]$ through Equation 2 can in principle be guessed purely intuitively with some physical considerations. However, in order to obtain more realistic values we extract those parameter values by first performing a DFT calculation, then extract the tight-binding parameters from the DFT result using a computational package called Wannier90 [8].

To solve our model, we use a standard many-body approach that relies on Green's functions. For our particular purpose, we work with retarded Green's function defined in matrix form through the Dyson equation

$$[G^R(\vec{k},\omega)] = \left[(\omega + i0^+)[I] - [H_0(\vec{k})] - [\Sigma(\vec{k},\omega)]\right]^{-1}. \tag{8}$$

Here the mean-field treatment implies that self-energy matrix becomes independent of both $\vec{k}$ and ω, that is,

$$[\Sigma(\vec{k},\omega)] \approx [\Sigma]. \tag{9}$$

$[\Sigma]$ depends on the average occupation numbers of electrons of the *d*-orbitals as the manifestation of the mean-field treatment of the second and third terms of the Hamiltonian defined in Equation 1. Thus, the average occupation numbers of electrons of the *d*-orbitals, and hence, also the self-energy matrix, are to be calculated self-consistently, starting with some initial guesses. For this purpose the parameters J_H and U are to be determined a priori.

During the iteration process we need to calculation both the partial density of states (PDOS) and the total density of states (DOS) of the system, respectively, as

$$\mathrm{PDOS}(\omega) = -\frac{1}{\pi}\frac{1}{N}\sum_{\vec{k}} \mathrm{Im}\, G_{\alpha\alpha}^R(\vec{k},\omega), \tag{10}$$

$$\mathrm{DOS}(\omega) = -\frac{1}{\pi}\frac{1}{N}\sum_{\vec{k}} \mathrm{Im\ Tr}\left[G^R(\vec{k},\omega)\right]. \tag{11}$$

N is the total number of $\vec{k}$-points in the Brillouin zone, which is equal to the number of unit cells in the system. Further, we need to determine the chemical potential, μ, of the system by imposing the appropriate total number of valence electrons, n_{total}, as a constraint, that is

$$n_{\mathrm{total}} = \int_{-\infty}^{\infty} d\omega\, \mathrm{DOS}(\omega) f(\omega, T, \mu), \tag{12}$$

with $f(\omega, T, \mu)$ denoting the Fermi-Dirac distribution function defined as

$$f(\omega, T, \mu) = \frac{1}{e^{\frac{\omega-\mu}{k_B T}}+1}. \tag{13}$$

The obtained chemical potential is then used to re-compute the spin-resolved average occupation numbers of the d-electrons

$$\langle n_{\alpha\uparrow(\downarrow)} \rangle = \int_{-\infty}^{\infty} d\omega\, \mathrm{PDOS}_{\alpha\uparrow(\downarrow)}(\omega) f(\omega, T, \mu), \tag{14}$$

which are then used to re-compute the self-energy matrix $[\Sigma]$. When the difference between the initial guess and the calculated value of $[\Sigma]$ is still bigger than some tolerance, some mixture of the initial guess and the calculated value of $[\Sigma]$ is used as a new initial guess, and then the process repeats back from Equation 8 to Equation 14. The cycle stops when the convergence is achieved.

After the self-consistency is achieved, we can calculate the net up and down electron spins of the system using equation

$$\langle n_{\uparrow(\downarrow)} \rangle = \int_{-\infty}^{\infty} d\omega\, \mathrm{DOS}_{\uparrow(\downarrow)}(\omega) f(\omega, T, \mu). \tag{15}$$

And finally, we calculate the magnetic moment of the system by the following equation

$$m = \langle n_{\uparrow} \rangle - \langle n_{\downarrow} \rangle. \tag{16}$$

For Fe_2MnAl structure, if we use the primitive unit cell, the resulting value of m already directly gives us the net magnetic moment value per formula unit of Fe_2MnAl in the unit of Bohr magneton, μ_B. The entire calculation process can be summarized in the following flow chart (Fig. 2).

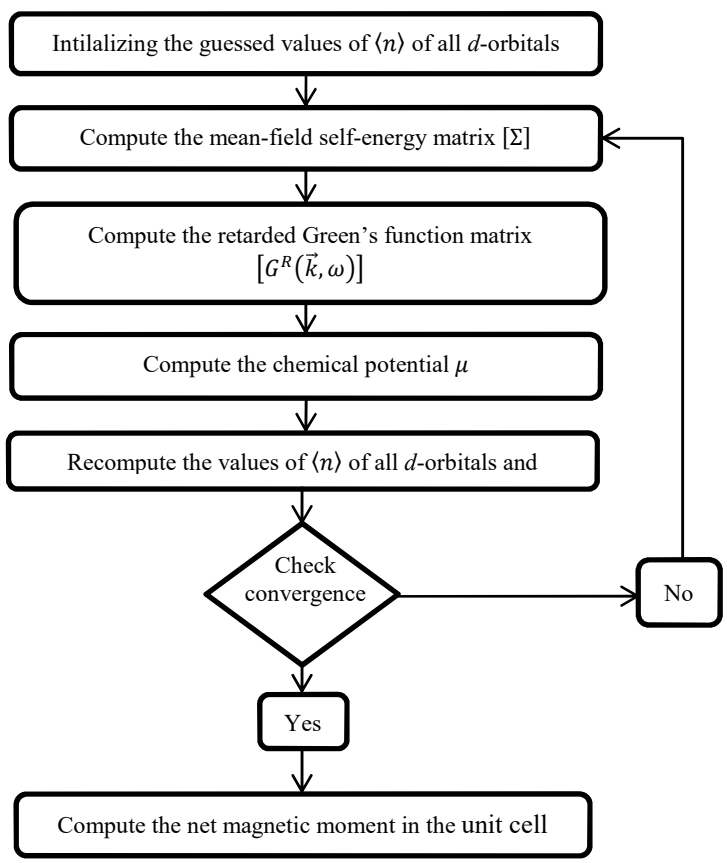

FIGURE 2. Mean-field algorithm.

SUMMARY

We have formulated the tight-binding based algorithm to calculate the net magnetic moment of Fe_2MnAl to be solved within mean-field approximation. Our next step is to develop the code and do the computation. The desired final results are to be compared with the existing experimental and other theoretical studies.

ACKNOWLEDGMENTS

We gratefully acknowledge and appreciate the funding support to this project from the Directorate of Research and Community Services of Universitas Indonesia though PITTA Research Grant No. 2021/UN2.R12/HKP.05.00/2016.

REFERENCES

1. C. Felser, L. Wollmann, S. Chadov, G. H. Fecher, and S. S. P. Parkin, APL Mater. **3**, 041518-1-041518-8 (2015).
2. F. Heusler, Verh Deutsche Physikalische Gesellschaft **5**, 219 (1903).
3. M. Belkhouane *et al.*, J. Magn. Magn. Mater. **377**, 211-214 (2015).
4. F. Dahmane *et al.*, J. Magn. Magn. Mater. **407**, 167-174 (2016).
5. T. Graf, C. Felser, and S. S. P. Parkin, Prog. Solid State Ch. **39**, 1-50 (2011).
6. T. Gasi *et al.*, Phys. Rev. B **87** 064411-1-064411-12 (2013).
7. D. Nanto, D.-S. Yang, and S.-C. Yu, Phys. B Condens. Matter **435**, 54-57 (2014).
8. A. A. Mostofi *et al.*, Comput. Phys. Commun. **185**, 2309-2310 (2014).